ARTICLE

Hybrid hydrogel films with graphene oxide for continuous saliva-level monitoring

Received 00th January 20xx,
Accepted 00th January 20xx

DOI: 10.1039/x0xx00000x
www.rsc.org/

Zifeng Zhang,[a, b] Qian Dou,[a, b] Shiwen Wang,[a] Debo Hu,[a] Xiangdong Guo,[a, c] Baoxin Liao,[a, c] Zhipeng Zhao,[a, c] Hongliang Liu*,[d] Qing Dai*[a, b, c]

Glucose-sensitive hydrogel coated on quartz crystal microbalance (QCM) sensor makes an important integrated system to realize continuous glucose monitoring system for diabetes, attributed to its high repeatability, rapid response time, and wide detection range. However, poor viscoelasticity of the functional hydrogel film usually leads to transport of water molecules out of the hydrogel matrix owing to the increased crosslinking density by molecular recognition, thus resulting in poor stability and limit of detection (LOD) of hydrogel-coated QCM sensor, which limits its practical application in the detection of low concentration of saliva glucose. Herein, this problem is solved by copolymerizing a rigid phenylboronic acid-containing graphene oxide (GO)-based monomer with a glucose-sensitive monomer (i.e., 3-acrylamidophenylboronic acid (3-APBA)) onto double bond-modified QCM chip to fabricate hybrid hydrogel-coated QCM sensor with improved viscoelasticity. Moreover, the 3-aminophenylboronic acid-grafted GO provides more reaction sites toward glucose, which is found to be beneficial to further improve the LOD of hydrogel-coated QCM sensor. The experimental results show that the LOD of the hybrid hydrogel film (1 mg L^{-1}) is about 10-fold and 900-fold lower than that of hydrogel film (10 mg/L) and polymer brushes (900 mg L^{-1}) respectively. This study provides a new approach for continuous sensing of saliva glucose using a highly sensitive hybrid hydrogel-coated QCM sensor with improved properties, which contributes to diagnosis, monitoring, and formulation of an appropriate treatment plan for patients suffering with diabetes.

1 Introduction

Use of the non-invasive continuous glucose monitoring (CGM) systems constitute the most promising method for the self-management of diabetes.[1–4] In recent years, extensive research efforts have been devoted to the study of non-invasive glucose monitoring. Body fluids such as saliva,[5, 6] sweat,[7–11] tears, or urine[12-14] act as potential candidates for direct measurement of glucose. Saliva has the advantages of being safe, convenient, and collectable in real time. Therefore, the detection of saliva glucose can be used as a method for continuous monitoring of diabetes.[15] Quartz crystal microbalance (QCM) is a highly sensitive, fast, and stable equipment, which is able to detect the subnanometer mass changes in the biosensors.[16–23] As a result, the sensing materials are key factors, which affect the properties of the QCM sensors. In general, rigid materials with good association with glucose act as promising candidates for constructing QCM-based glucose sensors. Nonetheless, glucose as a small molecule (molecular weight: 180.2 g/mol) might remain ineffective based on direct detection by the traditional rigid sensing materials, as its binding to the recognition molecules might not generate an obviously measurable change in the frequency. For example, Sugnaux and Klox[24] designed glucose-sensitive polymer brushes via direct surface reversible addition fragmentation chain-transfer polymerization; however, change in the frequency was found to occur at the high concentration of glucose (900 mg L^{-1}). As a consequence, Tang et al.[25] designed an amplified and facile QCM assay protocol for sensitive detection of glucose using concanavalin A (ConA) molecules as traces with a displacement-based mode on the rigid modified graphene film. However, the detection range was limited to 1.8–1350 mg L^{-1}, and the limit of detection (LOD) was 0.9 mg L^{-1} at the third harmonic resonance frequency (3δ) due to the limitation of ConA binding site. Moreover, the ConA molecules are susceptible to environmental factors including temperature, pH, humidity and ionic detergents, which make glucose-selective rigid graphene film-coated QCM sensor perform poorly. Therefore, studies on new material suitable for rapid and sensitive detection of saliva glucose are highly desirable.

Hydrogels are three-dimensional (3D) networks of hydrophilic polymers, which swell but do not dissolve in water. The advantage of most hydrogels include their easy functionalization to undergo a reversible change in response to external stimuli such as glucose, pH, ionic strength, biomolecule binding etc.[26–31] For example, the glucose-selective QCM sensors based on 3-acrylamidophenylboronic acid (3-APBA) functionalized hydrogel

[a] *Division of Nanophotonics, CAS Key Laboratory of Standardization and Measurement for Nanotechnology, CAS Center for Excellence in Nanoscience, National Center for Nanoscience and Technology, Beijing 100190, China*
[b] *School of Materials Science and Engineering, Zhengzhou University, Zhengzhou 450001, China*
[c] *Center of Materials Science and Optoelectronics Engineering, University of Chinese Academy of Sciences. Beijing 100049, China*
[d] *Technical Institute of Physics and Chemistry, University of Chinese Academy of Sciences. Beijing 100049, China*
**E-mail: daiq@nanoctr.cn, liuhl@mail.ipc.ac.cn*
†Electronic Supplementary Information (ESI) available: See DOI: 10.1039/x0xx00000x

exhibited high reusability and rapid response time, and realized the detection of physiological range of blood glucose concentration.[32] Although such a system exhibits a high performance, there are some crucial issues that must be addressed before detecting the low concentration of saliva glucose based on hydrogel-functionalized QCM sensor. These issues are as follows:[33] (1) the density of glucose in saliva is only 1 to 10% of that in the blood, thus such a low concentration cannot be detected quantitatively and continuously by using existing QCM sensor; (2) the poor viscoelasticity of hydrogel film, which causes the transport of water out of the matrix of the hydrogel film via molecular recognition, results in only partial coupling of the film to the vibration of the QCMs. This leads to a large fluctuation in frequency of QCM sensor, resulting in a poor stability problem and LOD of hydrogel-coated QCM sensor.

Therefore, in this study, in order to further improve the LOD and the stability of the hydrogel-functionalized QCM sensor, hybrid hydrogel films covalently bonded with phenylboronic acid-containing graphene oxide (GO) that meet the detection of saliva glucose in buffer solution were successfully fabricated, and their performance through QCM detection was thoroughly investigated. GO[34] has been proposed as an excellent filler for hydrogels due to its large surface area and outstanding physical, mechanical, and electrochemical properties. Moreover, various functional groups are present at the edges of GO (carboxyl) and at its basal planes (hydroxyl and epoxide), which leads to its easy functionalization. However, utilizing the advantages of GO by physical approach is limited due to poor compatibility between GO and polymer matrix.[36] Herein, 3-aminophenylboronic acid and double bond were introduced onto the GO via amidation and nucleophilic substitution to gain more reaction sites toward glucose, and in situ bound to the hydrogel to improve the compatibility between GO and polymeric matrix and viscoelasticity of hydrogel. The hybrid hydrogel film covalently bonded with rigid phenylboronic acid-containing functionalized GO (M-GO) was prepared in the presence of 3-APBA as the glucose-sensing component, and with acrylamide as the monomer and N,N-methylenebisacrylamide as the crosslinking agent via surface-initiated polymerization method. The hybrid hydrogel film with a LOD of 1 mg L^{-1} at fundamental frequency and good correlation (R^2 = 0.998) between $\triangle$f and $\triangle$m could be achieved at the low content of functionalized GO (ca. 0.48%). Our results demonstrated that the LOD and stability of hydrogel could be effectively improved by incorporating M-GO into the hydrogel matrix.

2 Experiment Section

Materials

Natural graphite flakes with an average diameter of 2.6 μm were supplied by Jinrilai graphite Co. Ltd. (Qingdao, China). Amberlite 732 and Amberlite IRA-4200 were purchased from Macklin. 0.2 μm PVDF blotting membranes were obtained from Sigma-Aldrich. Concentrated sulfuric acid (H_2SO_4, AR), sodium nitrate ($NaNO_3$, AR), potassium permanganate ($KMnO_4$, AR), hydrogen peroxide (H_2O_2, 30% aqueous solution), concentrated hydrochloric acid (HCl, 36–38%), barium chloride ($BaCl_2$, AR), sodium hydroxide (NaOH, AR), ethanol (C_2H_5OH, AR), dimethyl formamide (DMF, AR), and dimethyl sulfoxide (DMSO, AR) were purchased from Beijing Chemical Factory (China). 3-(Methacryloyloxy)propyltrimethoxysilane (KH570, 98%, Alfa Aesar), 3-aminophenylboronic acid (3-PBA, 98%, Alfa Aesar), 1-ethyl-3-[3-dimethylaminopropyl]carbodiimide (EDC, 98%, Alfa Aesar), N-hydroxysuccinimide (NHS, 98%, Alfa Aesar), N,N-methylenebisacrylamide (BIS, 98%, Sinopharm Chemical Reagent Co., Ltd.), 3-acrylamidophenylboronic acid (3-APBA, 98%, Frontier Scientific), acrylamide (AM, 98.5%, Xilong Chemical Industry Incorporated, Co., Ltd.), 2,2-dimethoxy-1,2-diphenylethanone (DMPA, >98%, Tokyo Chemical Industry) were also used in the experiments. Analytically pure reagents (glucose, sodium phosphate dibasic dodecahydrate, and potassium dihydrogen phosphate) were employed for carrying out the experiments. The saliva was collected from volunteers.

Chemical modification of GO with 3-PBA and KH570

GO was prepared based on a modified Hummers' method as previously reported.[35] Briefly, $NaNO_3$ (3 g) was added to pre-cooled (0 °C) concentrated H_2SO_4 (69 mL). After the dissolution of $NaNO_3$, natural graphite (3 g) was added to this $NaNO_3$/H_2SO_4 solution. Further, $KMnO_4$ (9 g) was then added gradually with stirring and the temperature of the mixture was maintained at below 5 °C. The mixture was then stirred at 35 °C for 30 min, and distilled water (138 mL) was slowly added to the mixture. Simultaneously, temperature was increased to 98 °C and then maintained for 15 min. The reaction was terminated by adding distilled water (420 mL) followed by the addition H_2O_2 solution (30 mL, 30%). The solid product was separated by centrifugation, and washed repeatedly with HCl solution (5%) until sulfate could not be detected by titration with $BaCl_2$ solution. The resultant GO was dried at 105 °C. GO (100 mg) was dispersed in prepared ethanol solution of EDC (0.4 M) and NHS (0.1 M) (1:1, v:v) via ultrasonication, and then 3-PBA (100 mg) and KH570 (200 μL) were added with mechanical stirring. The mixture was refluxed at 60 °C for 24 h, and then filtrated with organic membrane having an average pore size of 0.22 μm. The filtrated powder was further rinsed in ethanol (20 mL) with the aid of ultrasonication for 15 min and then filtrated. The rinsing-filtration process was repeated for 3 times. Finally, the resultant M-GO was dried at 105 °C for 2 h.

Surface modification of quartz chip

First, the quartz chips were sonicated in piranha solution (98% H_2SO_4:30% H_2O_2 = 7:3) for 10 min to eliminate organic substances, rinsed with distilled water, and dried under nitrogen. Then the quartz chip was incubated for 24 h in a 25 mL mixed solution in which the volume ratio of the KH570 and ethanol was about 1:250 to graft the double bond.

Fabrication of hybrid hydrogel films

First, the M-GO suspension in DMSO (1 mg/100 µL) was dropped into pre-polymer solution (200 µL, 1 mg/2 µL) consisting of 18% 3-APBA, 78% AM, 2% BIS, and 2% DMPA (by mass) in DMSO. The above mentioned mixture was then placed in the ultrasonication bath to obtain a pre-polymer solution with uniform dispersion. Second, the above mentioned mixture (30 µL) was deposited onto the upper electrode of the quartz chip and then quartz crystal was pressed with appropriate force. Third, the coated quartz crystals were exposed to UV irradiation (λ = 365 nm) under nitrogen atmosphere for 60 min for polymerization. Finally, the film-coated quartz chips were repeatedly rinsed with ethanol and distilled water. If the content of M-GO in the hybrid hydrogel was 0.48%, the film would be expressed as hybrid hydrogel-0.48%. Similarly, the hydrogel film containing 18% 3-APBA, 78% AM, 2% BIS, and 2% DMPA was prepared according to the above mentioned procedure for comparative analysis.

Verification of glucose sensitivity

A quartz chip coated with saliva glucose-sensitive hydrogel film was dried under nitrogen and installed into the flow cell of the QCM 200 system. PBS (0.1 mol L^{-1}) was continuously pumped into the flow cell, and the frequency of the crystal was monitored in real time by using the QCM data acquisition software. After the stabilization of frequency (frequency shift ≤ ±4 Hz), the glucose detection capacity of the materials was evaluated. Solutions (1.5 mL) with increasing and decreasing glucose concentration (from 0.0 to 36 mg L^{-1} with PBS, and then in reverse) were pumped into the flow cell every 5 min, and the frequency shift ΔF was recorded for each glucose concentration. Several cycles of these experiments were conducted at the pH = 7.5. Further experiments were conducted to verify the reversibility of the films by repeatedly pumping glucose solution with concentration of 0.0 and 20 mg L^{-1} into the flow cell.

Characterization

IR transmission measurements were performed by FTIR spectroscopy (Thermo Fisher Nicolet iN10). Raman spectroscopy was performed using a Horiba Jobin Yvon LabRAM HR800 microscope. AFM measurements were conducted using a scattering Snom microscope (Neaspec GmbH). Surface morphology and cross-section of freeze-fractured hydrogel and hybrid hydrogel were characterized by SEM (Hitachi S-4800). The viscoelastic properties of hydrogel and hybrid hydrogel were determined via dynamic thermomechanical analysis using Q800 instrument. The rheological analysis at 0.3% strain recorded the storage modulus and loss modulus versus frequency to monitor the mechanical properties of the hydrogel and hybrid hydrogel. WCA was obtained on a dynamic/static contact angle instrument at 25 °C, by the sessile drop method with 3 water droplets. The QCM measurements were carried out using an SRS-QCM 200 instrument (fundamental frequency of 5 MHz).

3 Results and Discussion

Figure 1a demonstrates the immobilization of the hybrid hydrogel films onto a quartz chip by surface-initiated polymerization. Briefly, M-GO and prepolymer solution were coated on the double bond-modified quartz chip, and then quartz crystal was pressed with appropriate force to form a homogeneous liquid layer. The hybrid hydrogel film was synthesized by ultraviolet (UV)-initiated free-radical polymerization. Figures 1a (I–III) show the structures of double bond-modified quartz chip, M-GO, and hybrid hydrogel. According to the ratio of the added PBA and KH550, the modified ratio was found to be approximately 1:1 on GO. The detail procedure for synthesis of hybrid hydrogel film is presented in Figure S1. Schematic illustration of the binding of hydrogel and hybrid hydrogel to glucose is presented in Figure1b. Earlier studies have shown that the interaction of immobilized PBAs in hydrogel matrix with low concentration of glucose can lead to volumetric shrinking of hydrogel.[37] Figure 1b-I indicates that the interaction of hydrogel with glucose caused the volumetric shrink, and as a result, the water was transported outside the hydrogel matrix. This could cause a large fluctuation in frequency of QCM sensor, resulting in a poor stability problem and LOD of hydrogel-coated QCM sensor. Compared to hydrogel, the interaction of hybrid hydrogel with glucose resulted in smaller volumetric change; therefore, there was almost no transport of water in hybrid hydrogel. This could be attributed to the improvement in the viscoelasticity of hydrogel due to the introduction of M-GO.

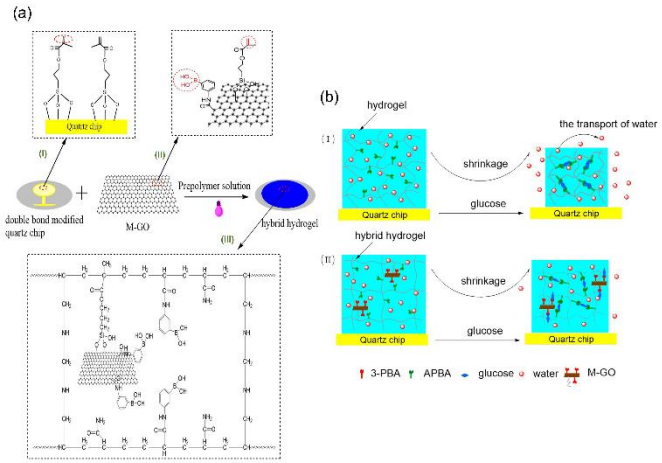

Figure 1. (a) The synthesis of hybrid hydrogel-coated QCM sensor, which was obtained by copolymerization of double bond-modified QCM chip with a rigid M-GO-based monomer and a glucose-sensitive monomer (i.e., 3-APBA); (b) A schematic diagram of the binding of hydrogel and hybrid hydrogel to glucose. Obvious volumetric shrinkage for hydrogel-coated QCM sensor, while much smaller volumetric change for hybrid hydrogel-coated QCM sensor;

The chemical structures of GO, M-GO, hydrogel, and hybrid hydrogel were characterized by fourier transform infrared (FTIR) spectroscopy and the corresponding FTIR spectra are shown in Figure 2a. The characteristic peaks at 1720, 1620, 1230, and 1050 cm^{-1} in FTIR spectrum of GO are ascribed to the stretching of C=O in carboxyl group, C=C in aromatic ring, C–O–C in epoxide group, and C–O in hydroxyl group, respectively.[38, 39] After the reaction of GO with 3-PBA and KH570, the characteristic peak at 1720 cm^{-1} becomes gradually weak and the two characteristic peaks are

simultaneously generated at 1580 and 1170 cm^{-1}, corresponding to the deformation vibrations of N–H and the stretching vibrations of C–N in secondary amide, respectively, indicating the reaction of carboxyl group with 3-PBA via amidation. On the other hand, the characteristic peak at 1230 cm^{-1} for C–O–C in epoxide group disappeared and the characteristic peak at 705 cm^{-1} for the deformation vibration of N–H in secondary amine appeared, which demonstrates that the epoxide groups reacted with 3-PBA via nucleophilic substitution reaction. Moreover, peak for the stretching vibrations of C–H is located at 2920 cm^{-1}, which indicates the successful introduction of KH570 onto the surface of the GO. Compared to the FTIR spectrum of hydrogel, FTIR spectrum of hybrid hydrogel exhibits the existence of the characteristic peak at 1180 cm^{-1} for C–N in secondary amide corresponding to the peak of M–GO chain. Moreover, the intensity of peak at 1540 cm^{-1} corresponding to the deformation vibrations of N–H in secondary amide was reduced due to the steric hindrance of M-GO. Finally, presence of the characteristic peak of $–B(OH)_2$ at 1360 cm^{-1} indicates the deposition of hybrid hydrogel. In order to further approve the introduction of M-GO into the hydrogel, the Raman spectra of M-GO, hydrogel, and hybrid hydrogel were obtained and presented in Figure 2b. Raman spectrum of M-GO displays a prominent G Peak at 1569 cm^{-1}, corresponding to the first-order scattering of the E2g mode. Furthermore, the prominent D band is observed at 1329 cm^{-1}, indicating the reduction in size of the in-plane sp2 domains, possibly due to the extensive oxidation.[40] Compared to the Raman spectrum of hydrogel, the Raman spectrum of hybrid hydrogel contains both G and D bands. The results of FTIR and Raman spectroscopy indicate the successful introduction of M-GO into the hydrogel. Furthermore, the thickness of the film (Fig.2) is an important parameter that dictates the performance of the hybrid hydrogel film. The atomic force microscopy (AFM) image and thickness of hybrid hydrogel film are shown in Figures 2c and 2d. The experiments indicated that the results have high sensitivity, low detection limit, superior recovery, and correlation coefficients when hybrid film thickness is approximately 700 nm. Compared to the thickness of hydrogel film shown in Figure S2 (ca. 200 nm), the thickness of hybrid hydrogel film is more at the same pressure. This could be attributed to the exfoliated layers of M-GO in the hydrogel matrix. In order to further investigate the micromorphology of the hybrid hydrogel and filler (graphene nanosheets) dispersion in the film, scanning electron microscopy (SEM) characterization was carried out to observe the surface of the film. Figures 2e and 2f demonstrate that the typical SEM images show a flat surface of hydrogel film and hybrid hydrogel film. Compared to the hydrogel film, the exfoliated layers of M-GO can be observed in the hybrid hydrogel matrix. The red circle in Figure 2f shows cleavage planes-oriented parallel arrangement of M-GO to their surfaces and similar phenomenon can be observed in the hybrid hydrogel-0.6% film (Figure S3). This indicates the dispersion of the M-GO sheets in hybrid hydrogel film with a certain direction in the entire body.

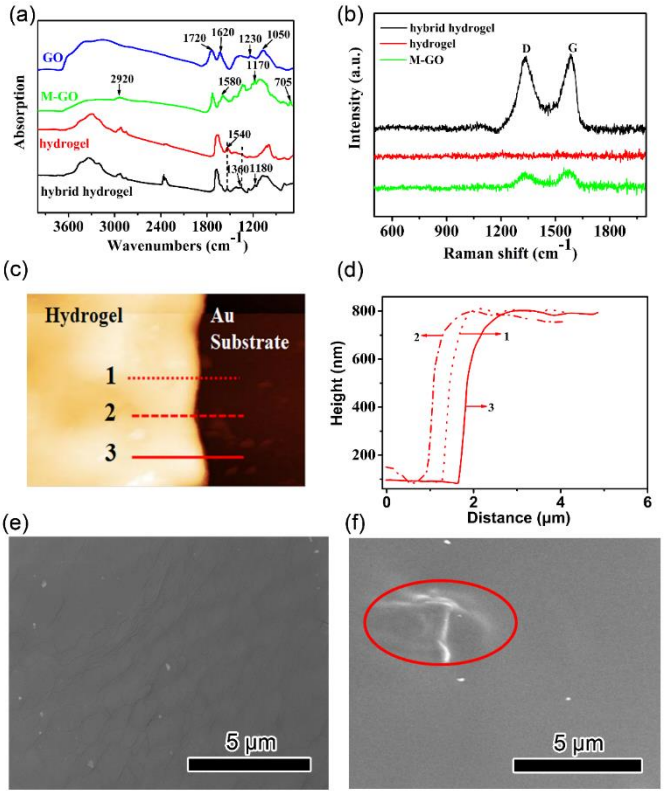

Figure 2. (a) FTIR spectra of GO, M-GO, hydrogel, hybrid hydrogel; (b) Raman spectra of M-GO, hydrogel, hybrid hydrogel, obtained using a 514 nm excitation wavelength; (c) The AFM image of hybrid hydrogel film; (d) The thickness of hybrid hydrogel film. SEM image of (e) hydrogel and (f) hybrid hydrogel.

Figure 3 shows the sensitivity, LOD, and reusability of hybrid hydrogel film based on QCM sensor to identify glucose. Figure 3a illustrates that the hybrid hydrogel film based on QCM sensor reveals high stability with several frequency shifts of 2.5 Hz (the fundamental frequency of this QCM system is 5×10^6 Hz, only 0.5 ppm of the fundamental frequency) over 120 min at pH = 7.5 phosphate buffer saline (PBS) solution; however, the hydrogel film based on QCM sensor shows frequency shift of about 6.5 Hz (Figure S4). This demonstrates that the hybrid hydrogel film-coated QCM sensor was more stable than the hydrogel film-coated QCM sensor. The clinical studies employing the classic spectroscopic methods have reported saliva glucose concentrations of around 11.8 $\pm$ 6.75 mg L^{-1} for healthy individuals and 49.5 $\pm$ 24.8 mg L^{-1} for the diabetic individuals.[41] Wang et al. prepared a disposable electrochemical sensor, and found that the saliva glucose level in healthy people is below 20 mg L^{-1}.[42] Yan et al. prepared organic electrochemical transistors with the gate electrodes modified with a polyaniline (PANI)/nafion-graphene bilayer film, and they found saliva glucose levels in healthy people to be in the range of 16.74–20.34 mg L^{-1}.[43] Sener et al. used the hexokinase method to study the saliva levels, and they found the glucose levels in healthy person to be in the range of 13.25–15.34 mg L^{-1} in unstimulated saliva.[44] However, low saliva glucose solution in healthy individuals (<10 mg L^{-1}) cannot be detected using existing QCM sensor. Therefore, the 0–36 mg L^{-1} glucose solution was selected to study the glucose sensitivity in this study.

The response and recovery behaviour is important for evaluating the dynamical performance of a QCM glucose sensor. Figure 3b shows that the hybrid hydrogel film responds to glucose concentration ranging from 0.0 to 36 mg L^{-1}. When solution with increasing concentration of glucose was pumped into the flow cell, the fundamental frequency of the quartz-hybrid hydrogel complex resonator decreased due to the association of glucose molecules with the hybrid hydrogel matrix. In contrast, when solution with decreasing concentration of glucose was pumped into the flow cell, the fundamental frequency of the quartz-hybrid hydrogel complex resonator exhibited an increasing trend due to the dissociation of glucose molecules from the hybrid hydrogel, reaching the maximum at glucose-free solution, which indicated that the dynamic range of hybrid hydrogel film based QCM sensor is broad enough to cover the saliva glucose levels in healthy people. Braun et al.[37] reported that the fast response kinetics (response time) of biosensor is an important attribute for glucose monitoring, in particular, continuous glucose monitoring. Their experimental results showed that the hydrogel composed of polymerized crystalline colloidal arrays (PCCA) modified with phenylboronic acid possessed response time of 100 min, which indicated that the hydrogel facilitated the achievement of continuous glucose monitoring. Koschinsky and Heinemann[45] reported that the response time of ideal continuous glucose monitoring should not exceed 5 min. In this study, the response time (the time span during which the QCM frequency shift reaches the 90% limit between two successive glucose concentration steps) of hybrid hydrogel was less than 5 min (see Figure 3b). Therefore, our results demonstrated that the hybrid hydrogel-coated QCM sensor could achieve continuous saliva glucose monitoring.

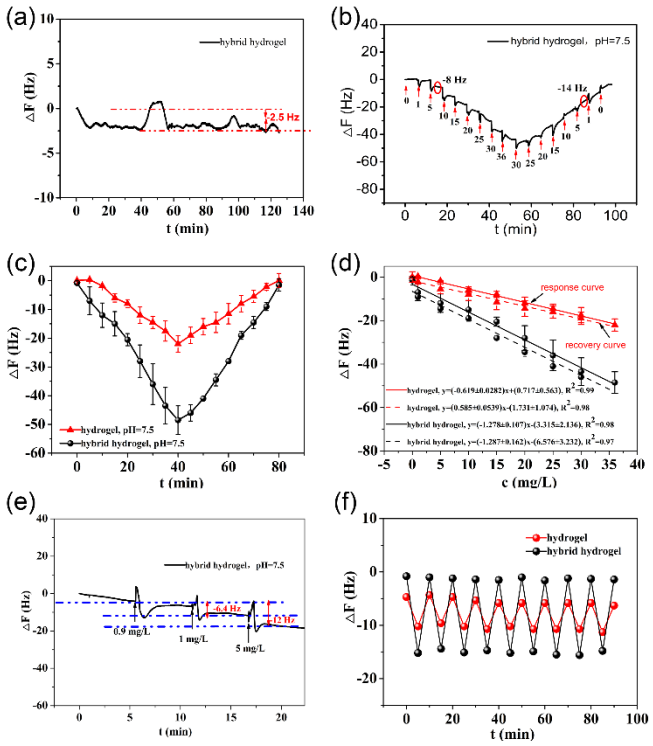

Figure 3. The sensitivity, LOD and repeatability of hybrid hydrogel film based on QCM sensor to identify glucose. (a) The stability of hybrid hydrogel film coated on QCM sensor in PBS solution at pH=7.5; (b) Response and recovery curves of hybrid hydrogel film based on QCM sensor at pH=7.5; (c) Glucose sensitivity of hydrogel and hybrid hydrogel film at pH=7.5; (d) Relationship response and recovery behavior between frequency shift and glucose concentration; (e) The low detection limit of hybrid hydrogel film coated on QCM sensor; (f) Repeatability of hybrid hydrogel film and hydrogel film based on QCM sensor.

Different responses of frequency shift to 5 mg L^{-1} (response frequency shift: –8 Hz, recovery frequency shift: –14 Hz) are caused by the hysteresis in the recovery process, which is attributed to the slow response kinetics.[37] However, the slight hysteresis does not affect the dynamic glucose detection of hybrid hydrogel-coated QCM sensor, because the glucose levels of recovery process still can be derived by the recovery behavior between frequency shift and glucose concentration as presented in Figure 3d. Figure 3c shows glucose response of the hydrogel and hybrid hydrogel film at pH = 7.5. When the glucose concentration was increased to 36 mg L^{-1}, the total frequency of hydrogel and hybrid hydrogel film was found to shift by 20 and 52 Hz, respectively. Figure 3d demonstrates that the frequency shift of response and recovery behaviour is linearly proportional to the glucose concentration over the range of 0.0–36 mg L^{-1}. The response and recovery correlation coefficients of hydrogel and hybrid hydrogel were 0.99, 0.98, 0.98 and 0.97, respectively, which indicated hydrogel and hybrid hydrogel correlated well with the required glucose concentration in saliva. Moreover, in case of the hybrid hydrogel film, hydrophobicity and existence of rigid M-GO in the network structure of hydrogel can prevent the transport of water in the hybrid film. The lowest concentration of glucose solution that could be detected by our system was identified and the result is shown in Figure 3e. Clearly, with the increase in the glucose concentration to 1 mg L^{-1}, the hybrid hydrogel film begins to respond with a frequency shift of 6.4 Hz. Therefore, the hybrid hydrogel film coated on the QCM sensor has a LOD of 1 mg L^{-1} at the fundamental frequency, which is sufficient to be applicable for typical saliva glucose monitoring. Noteworthy, compared to the LOD (10 mg L^{-1}) of hydrogel film shown in Figure S5, the hybrid hydrogel film has a lower LOD. The values of LOD of hybrid hydrogel, hydrogel, and polymer brushes are shown in Figure S6. Hybrid hydrogel has a LOD nearly 10-fold and 900-fold lower than those of hydrogel and polymer brushes, respectively, which exhibited excellent LOD. The repeatability of the hydrogel and hybrid hydrogel film was tested by alternately pumping solution with pH = 7.5 PBS (glucose-free solution) and 20 mg/L glucose solution into the flow cell (Figure 3f). After nine association–dissociation cycles, the hydrogel film and hybrid hydrogel film maintained their glucose sensitivity, thus showing good repeatability of the QCM sensor toward glucose. Table S1 presents that the hydrogel film and hybrid hydrogel film possessed the relative standard deviations (% RSD) of 4.6 and 2.6% (n = 9), respectively, which further demonstrated that the hydrogel and hybrid hydrogel-coated QCM sensor showed a good repeatability. The improvement in the sensitivity, LOD, and stability of hybrid hydrogel is attributed to the following reasons: (1) the phenylboronic acid-containing GO covalently bonded to the hydrogel enables more reaction sites toward glucose molecules and (2) the hydrophobic and rigid M-GO improves the viscoelasticity of

hydrogel matrix, thereby preventing the transport of water present in the hydrogel matrix.

In order to further verify the effects of M-GO on the structure of hydrogel film, the cross-sectional SEM images of freeze-fractured hydrogel and hybrid hydrogel film were obtained as shown in Figures 4a and 4b. The hybrid hydrogel film reveals a more compact and ordered lamellar structure than hydrogel film, which is attributed to the in-situ binding of the M-GO to the hydrogel matrix. Importantly, the compact structure of hydrogel can transfer stress and constrain the movement of the molecular chain, thereby enhancing the strength and rigidity of the hydrogel matrix and improving the stability of QCM sensor. Figure 4c shows the storage and loss moduli of hydrogel and hybrid hydrogel. The hybrid hydrogel has higher values of storage moduli (G') and loss moduli (G") than the hydrogel, which indicates that the M-GO contributes to increasing the intermolecular force and stabilizing the polymer chain network structure, thereby improving the viscoelastic performance of the hydrogel. The water contact angles (WCAs) of hydrogel and hybrid hydrogel were measured by water droplet method (Figure 4d). After the introduction of M-GO, the contact angle of hydrogel was increased from 66° to 83°, which was ascribed to the hydrophobic nature of M-GO. Hybrid hydrogel exhibited hydrophobicity and excellent mechanical properties, which indicated that the introduction of M-GO could effectively prevent the transport of water in the hydrogel and provide more reaction sites. Therefore, the hybrid hydrogel film coated on QCM sensor showed excellent stability and lower LOD. The saliva contains many biological chemicals which are adverse factors that can limit the sensitivity and accuracy of QCM sensor.[46] To eliminate the non-specific adsorption of biological chemicals on the QCM sensor, first, the saliva samples were boiled at 100 °C for 30 min to remove most of protein; then PVDF membrane and ion exchange resin were used to further filter out most of proteins and ions in saliva. Figures S7a and b illustrate that after several steps of treatment, the color of saliva changed from yellow to transparent, which demonstrated successful elimination of most of biological chemicals. Figure S7c exhibits that the response frequency shift of hybrid hydrogel-coated QCM sensor in treated saliva was 6.4-fold lower than that of hybrid hydrogel-coated QCM sensor in untreated saliva. This demonstrated significant reduction in the non-specific adsorption of biological chemicals in saliva, which was beneficial for the hybrid hydrogel to achieve the detection of saliva glucose in real human saliva. In the QCM based sensor, viscoelastic behavior is important parameters. Figure S8 exhibits that although the thickness of hybrid hydrogel film increased to 700 nm owing to the introduction of graphene oxide, there was still no obvious change in △R during glucose measurement, which demonstrated that there was also almost no change in viscoelasticity of hybrid hydrogel film.[47]

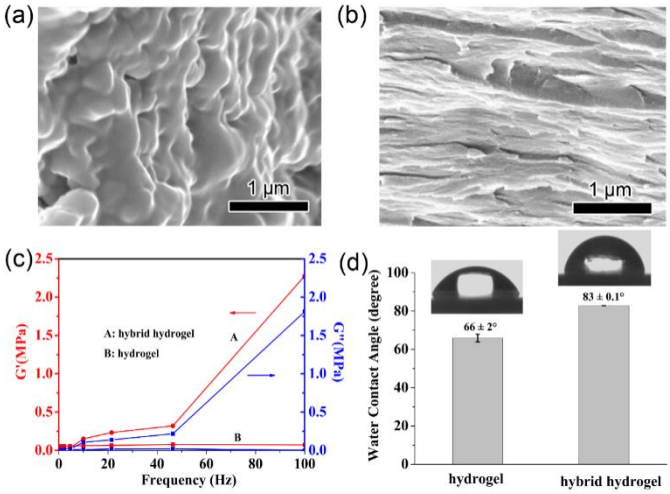

Figure 4. SEM image of cross-sectional (a) hydrogel and (b) hybrid hydrogel; (c) storage and loss moduli of hydrogel and hybrid hydrogel as a function of frequency at room temperature; (d) water contact angles of hydrogel and hybrid hydrogel.

4 Conclusions

A glucose-selective hydrogel covalently bonded with phenylboronic acid-containing graphene oxide was successfully synthesized. The hybrid hydrogel exhibited better stability, sensitivity, and lower LOD of 1 mg L^{-1} compared to hydrogel (LOD: 10 mg L^{-1}), which solved the problem of high LOD of hydrogel-coated QCM sensor. The excellent properties of hybrid hydrogel-coated QCM sensor are attributed to the following reason: introduction of rigid M-GO not only improved the viscoelasticity of hydrogel matrix, but also provided more reaction sites toward glucose molecules. It is believed that phenylboronic acid-containing graphene oxide may provide an important model for application of two-dimensional materials in glucose biosensor. These results indicate that the hybrid hydrogel exhibits significant potential as a sensitive glucose probe for non-invasive sensors for continuous monitoring of saliva glucose.

Conflicts of interest

There are no conflicts to declare.

Acknowledgements

This work is supported by Science and Technology Service Network Project (STS Program) of Chinese Academy of Sciences (KFJ-STS-ZDTP-063), the National Key Research and Development Program of China (2016YFA0201600). The Ministry of Science and Technology focused on the research of "early identification, early diagnosis and cutting point of diabetes risk factors" (2016YFC1305700), Jiangsu Provincial Basic Public Health Service Innovation Pilot Project (WDF15-967), Jiangsu Medical Device Industry Technology Innovation Center Joint Fund (SYC2018004).

Notes and references

1 S. Wild, C. Roglic, A. Green, R. Sicree and H. King, Diabetes care, 2004, **27**, 1047-1053.

2 D. C. Klonoff, L. Blonde, G. Cembrowski, A. R. Chacra, G. Charpentier, S. Colagiuri, G. Dailey, R. A. Gabbay, L. Heinemann, D. Kerr, A. Nicolucci, W. Polonsky, O. Schnell, R. Vigersky and J. F. Yale, J. Diabetes Sci. Technol., 2011, **5**, 1529-1548.

3 I. Mamkin, S. Ten, S. Bhandari and N. Ramchandani, J. Diabetes Sci. Technol., 2008, **2**, 882-889.

4 M. C. Torjman, N. Dalal and M. E. Goldberg, J. Diabetes Sci. Technol., 2008, **2**, 178-181.

5 W. Zhang, Y. Du and M. L. Wang, Sens. Biosens. Res., 2015, **4**, 23-29.

6 H. Lee, T. K. Choi, Y. B. Lee, H. R. Cho, R. Ghaffari, L. Wang, H. J. Choi, T. D. Chung, N. Lu, T. Hyeon, S. H. Choi and D. H. Kim, Nat. Nanotech., 2016, **11**, 566-572.

7 J. Heikenfeld, Electroanalysis, 2016, **28**, 1242-1249.

8 W. Gao, S. Emaninejad, D. H. Lien, G. A. Brooks, R. W. Davis and A. Javery, Nature, 2016, **529**, 509-514.

9 A. Koh, D. Kang, Y. Xue, S. Lee, J. Kim, Y. Huang and J. A. Rogers, Sci. Transl. Med., 2016, **8**, 366ra165.

10 H. Lee, C. Song, Y. S. Hong, M. S. Kim, H. R. Cho, T. Kang, K. Shin, S. H. Choi, T. Hyeon and D. H. Kim, Sci. Adv., 2017, **3**, e1601314.

11 Y. J. Hong, H. Lee, J. Kim, M. Lee, H. J. Choi, T. Hyeon and D. H. Kim, Adv. Funct. Mater., 2018, **28**, 1805754.

12 Q. Y. Yan, B. Peng, G. Su, B. E. Cohan, T. C. Major and M. E. Meyerhoff, Anal. Chem., 2011, **83**, 8341-8346.

13 H. Yao, A. J. Shum, M. Cowan, I. Lahdesmaki and B. A. Parviz, Biosens. Bioelectron., 2011, **26**, 3290-3296.

14 J. H. Park, J. H. Kim, S. Y. Kim, W. H. Cheong, J. Jang, Y. G. Park, F. Bien and J. U. Park, Sci. Adv., 2018, **4**, eaap9841.

15 P. Abikshyeet, V. Ramesh and N. Oza, Diabetes, Metab. Syndr. Obes.: Targets Ther., 2012, **5**, 149-154.

16 S K Vashist and P. Vashist, J. Sensors, 2011, **1**, 2011.

17 T. Zhou, K. A. Marx, M. Warren and H. Schulze, Biotechnol. Prog., 2000, **16**, 268-277.

18 R. E. Speight and M. A. Cooper, J. Mol. Recognit., 2012, **25**, 451-473.

19 C. Yao, T. Zhu, Y. Qi, Y. Zhao, H. Xia and W. Fu, Sensors, 2010, **10**, 5859-5871.

20 K. A. Marx, Biomacromolecules, 2003, **4**, 1099-1120.

21 M. Lazerges, H. Perrot, N. Rabehagasoa and C. Comepere, Biosensors, 2012, **2**, 245-254.

22 Y. Tsuge, Y. Moriyama, Y. Tokura and S. Shiratori, Anal. Chem., 2016, **88**, 10744-10750.

23 D D Erbahar, I Gürol, F Zelder and M. Harbeck, Sens. Actuators, B, 2015, **207**, 297-302.

24 C, Sugnaux and H. A. Klok, Macromol. Rapid Commun., 2014, **35**, 1402-1407.

25 D. P. Tang, Q. F. Li, J. Tang, B. L. Su and G. N. Chen, Anal. Chim. Acta, 2011, **686**, 144-149.

26 V. L. Alexeev, A. C. Sharma, A. V. Goponenko, S. Das, I. K. Lednev, C. S. Wilcox, D. N. Frinegold and S. A. Asher, Anal. Chem., 2003, **75**, 2316-2323.

27 I. Cobo, M. Li, B. S. Sumerlin and S. Perrier, Nat. Mater., 2015, **14**, 143-159.

28 V. L. Alexeev, S. Das, D. N. Finegold and S. A. Asher, Clin. Chem., 2004, **50**, 2353-2360.

29 J. Huang, X. Hu, W. Zhang, Y. Zhang and G. Li, Colloid Polym. Sci., 2008, **286**, 113-118.

30 A. Giuri, S. Masi, S. Colella, A. Kovtun, S. D. Elce, E. Treossi, A. Liscio, C. E. Corcione, A. Rizzo and A. Listorti, Adv. Funct. Mater., 2016, **26**, 6985-6994.

31 C. K. Lim, Y. D. Lee, J. Na, J. M. Oh, S. Her, K. Kim, K. Choi, S. Kim and I. C. Kwon, Adv. Funct. Mater., 2010, **20**, 2644-2648.

32 Q. Dou, D. B. Hu, H. K. Gao, Y. M. Zhang, A. K. Yetisen, H. D. Butt, J. Wang, G. J. Nie and Q. Dai, RSC Adv., 2017, **7**, 41384-41390.

33 Y. H. Chen, S. Y. Lu, S. S. Zhang, Y. Li, Z. Qu, Y. Chen, B. W. Lu, X. Y. Wang and X. Feng, Sci. Adv., 2017, **3**, e1701629.

34 S. S. Stankovich, D. A. Dikin, R. D. Piner, K. A. Kohlhaas, A. Kleinhammes, Y. Y. Jia, Y. Wu, S. T. Nguyen and R. S. Ruoff, Carbon, 2007, **45**, 1558.

35 W. S. Hummers Jr and R. E. Offeman, J. Am. Chem. Soc., 1958, **80**, 1339-1339.

36 Z. H. Mo, R. Yang, S. Hong and Y. X. Wu, Int. J. Hydrogen Energy, 2018, **43**, 1790-1804.

37 C. Zhang, M. D. Losego and P. V. Braun, Chem. Mater., 2013, **25**, 3239-3250.

38 O. C. Compton, D. A. Dikin, K. W. Putz, L. C. Brinson and S. T. Nguyen, Adv. Mater., 2010, **22**, 892-896.

39 H. Tang, G. J. Ehlert, Y. Lin and H. A. Sodano, Nano Lett., 2012, **12**, 84-90.

40 A. C. Ferrari, J. C. Meyer, V. Scardaci, C. Casiraghi, M. Lazzeri, F. Mauri, S. Piscanec, D. Jiang, K. S. Novoselov, S. Roth and A. K. Geim, Phys. Rev. Lett., 2006, **97**, 187401.

41 Luis A. S. Jimenez, A. M. Lucero, V. Osuna, I. E. Moreno and R. B. Dominguez, Sensors, 2018, **18**, 1071.

42 Y. Du, W. J. Zhang and M. L. Wang, Biosensors, 2016, **6**, 10.

43 C. Z. Liao, C. H. Mak, M. Zhang, Helen L. W. Chan and F. Yan, Adv. Mater., 2015, **27**, 676-681.

44 C. Jurysta, N. Bulur, B. Oguzhan, I. Satman, T. M. Yilmaz, W. J. Malaisse and A. Sener, J. Biomed. Biotechnol., 2009, 430426.

45 T. Koschinsky and L. Heinemann, Diabetes Metab, Res. Rev., 2001, **17**, 113-123.

46 A. Hucknall, S. Rangarajan and A. Chilkoti, Adv. Mater., 2009, 21, 2441-2446.

47 M. J. Brown, A. R. Hillman, A. J. Martin, R. W. Cernosek and H. L. Bandey, J. Mater. Chem., 2000, 10, 115-126.

TOC Graphic

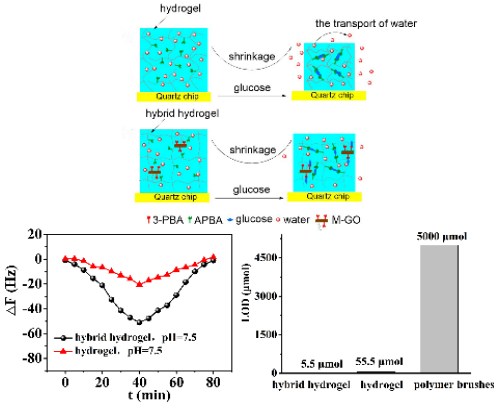
hydrogel
the transport of water
shrinkage
glucose
Quartz chip
Quartz chip
hybrid hydrogel
shrinkage
glucose
Quartz chip
Quartz chip
3-PBA
APBA
glucose
water
M-GO
ΔF (Hz)
t (min)
hybrid hydrogel, pH=7.5
hydrogel, pH=7.5
LOD (μmol)
5000 μmol
5.5 μmol
55.5 μmol
hybrid hydrogel
hydrogel
polymer brushes